Inorganic Chemistry

Article

pubs.acs.org/IC

Highly Reduced Double-Decker Single-Molecule Magnets Exhibiting Slow Magnetic Relaxation

Mathieu Gonidec,[†,‡] Itana Krivokapic,[#] Jose Vidal-Gancedo,[†,‡] E. Stephen Davies,[⊥] Jonathan McMaster,[⊥] Sergiu M. Gorun,*[,§] and Jaume Veciana*[,†,‡]

[†]Institut de Ciència de Materials de Barcelona (ICMAB-CSIC), 08193 Bellaterra, Spain

[‡]Networking Center on Bioengineering, Biomaterials and Nanomedicine (CIBER-BBN), 08193 Bellaterra, Spain

[§]Department of Chemistry and Biochemistry, Seton Hall University, 400 South Orange Avenue, South Orange, New Jersey 07079, United States

[⊥]School of Chemistry, University of Nottingham, Nottingham, NG7 2RD, U.K.

[#]Max Planck Institute for Bioinorganic Chemistry, Stiftstrasse 34-36, 45470 Mülheim an der Ruhr, Germany

Supporting Information

ABSTRACT: $F_{64}Pc_2Ln$ ($\mathbf{1}_{Ln}$, Ln = Tb or Lu) represent the first halogenated phthalocyanine double-decker lanthanide complexes, and $\mathbf{1}_{Tb}$ exhibits single-molecule magnet properties as revealed by solid-state magnetometry. The fluorine substituents of the phthalocyanine rings have a dramatic effect on the redox properties of the $F_{64}Pc_2Ln$ complexes, namely, a stabilization of their reduced states. Electrochemical and spectroelectrochemical measurements demonstrate that the $\mathbf{1}_{Tb}^{-/2-}$ and $\mathbf{1}_{Tb}^{2-/3-}$ couples exhibit redox reversibility and that the $\mathbf{1}_{Tb}^{-}$, $\mathbf{1}_{Tb}^{2-}$ and $\mathbf{1}_{Tb}^{3-}$ species may be prepared by bulk electrolysis in acetone. Low-temperature MCD studies reveal for the first time magnetization hystereses for the super-reduced dianionic and trianionic states of Pc_2Ln.

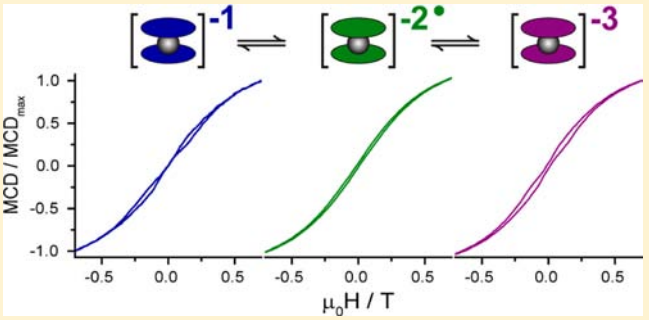

INTRODUCTION

The fact that single molecules can function as magnets[1] has triggered significant research efforts aimed at understanding their quantum properties and their exploitation in technological applications such as quantum information processing[2] or molecular spintronics.[3−6] Since the discovery of the first single-molecule magnet (SMM) in the early 1990s,[7−16] a massive synthetic effort has led to an extensive knowledge of this area based on an ever increasing number of compounds that exhibit this behavior.[17−27] A particularly appealing class of molecules for potential technological applications is that of the so-called double-decker phthalocyanine lanthanide complexes, Pc_2Ln.[7,28−30] This system (Figure 1), is based on single metal ions coordinated by two phthalocyanine macrocyclic ligands that exhibit a high chemical and thermal stability while being able to coordinate a wide range of metal ions. In addition, the ligands exhibit a rich electrochemistry and can be either oxidized or reduced while the central lanthanide ion maintains its 3+ oxidation state.

A distinct advantage of the phthalocyanine-based SMMs is that a wide range of substituents may be introduced at the periphery of the phthalocyanine macrocycles without significantly interfering with the metal binding properties of the ligands. The choice of the organic substituents and that of the lanthanide ion constitute two quasi-independent degrees of freedom that allow the synthesis of molecules with tunable properties. Thus, the variation of the lanthanide ion can lead to Pc_2Ln complexes exhibiting a wide range of electronic structures.[31]

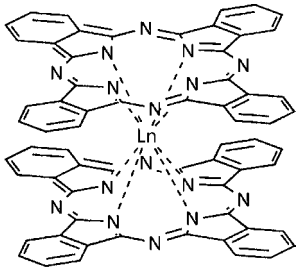

Pc_2Ln

Figure 1. Molecular structure of Pc_2Ln complexes.

In addition, Pc_2Ln complexes possess large magnetic anisotropies, which lead to relatively high activation barriers for the reversal of the magnetization (for example, the activation barrier for Pc_2Tb is ca. 420 cm^{-1}).[30] This property

Received: December 13, 2012
Published: March 29, 2013

   dx.doi.org/10.1021/ic3027418 | *Inorg. Chem.* 2013, 52, 4464−4471

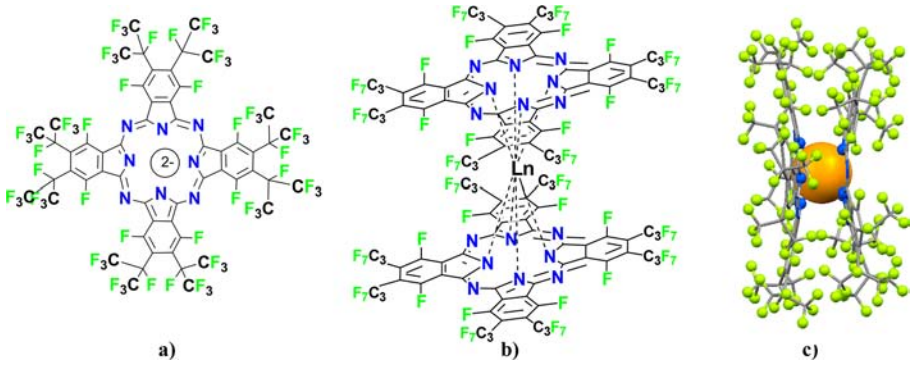

Figure 2. (a) The dianion of 1,4,8,11,15,18,22,25-octakis-fluoro-2,3,9,10,16,17,23,24-octakis-perfluoro (isopropyl)phthalocyanine, $F_{64}PcH_2$. (b) $F_{64}Pc_2Ln$ ($\mathbf{1}_{Ln}$), where Ln = Lu, Tb. (c) The single-crystal X-ray structure of $\mathbf{1}_{Ln}\mathbf{H}$ (Ln = Tb) viewed perpendicular to the ligands' 4-fold axis. The metal is represented as a van der Waals sphere. The rest of the structure is shown as ball-and-sticks. Color codes: metal center, orange; C, black; N, blue, F, green.

makes Pc_2Ln complexes ideal candidates for technological applications. Importantly, double-decker phthalocyanine lanthanide complexes have been shown to maintain their magnetic properties while in close vicinity to a surface,[32−36] a prerequisite for applications in molecular spintronics devices.

All Pc_2Tb complexes reported to date are based on Pc ligands containing C−H bonds, a feature which renders the molecules susceptible to chemical oxidation and raises questions about their long-term stability. Among the range of available oxidation states, $Pc_2Tb^{+/0/-}$ complexes have been shown to possess SMM properties at low temperature in bulk and in frozen dilute solutions,[7,31,37−41] but the doubly and triply reduced species could not be characterized magnetically due to their poor stability. Considering all of the above, Pc_2Ln that are resistant to chemical degradation and that may exhibit new redox states are desirable.

We report herein a new series of Pc_2Ln complexes that, for the first time, do not contain C−H bonds. Instead, the ligands exhibit C−F bonds segregated into aromatic and aliphatic ones in an 8:56 ratio.[42]

The aliphatic bonds, present in the perfluoroisopropyl substituents, play a key role in the stabilization of the fluorinated metal complexes, since, as recognized previously for single-decker transition metal phthalocyanine complexes, the lack of π-back bonding ability of the aliphatic fluorine substituents, unlike the aromatic ones, results in an enhanced electronic withdrawing effect to the point of suppressing the ability of the fluorinated phthalocyanines to be oxidized, whether the metal center is a main group[43] or a transition metal.[44] Perfluorinated single decker complexes can be reduced in solution[44−46] and in the solid state.[47]

The lack of oxidation is complemented by the lack of molecular degradation of C−F bonds during molecular oxygen-based catalysis,[48] as well as in the presence of activated oxygen species such as singlet oxygen[43,49,50] or by S-centered radicals.[51] Thus, the zinc and cobalt complexes of fluorinated phthalocyanines were shown to catalyze oxygenations via the production and incorporation of singlet-oxygen in organic substrates, as well as oxidations by the removal of hydrogen as water from C−H[48] and S−H bonds,[51] respectively.

Taken together, the fluorine substituents were anticipated to impart similar properties to lanthanide double-decker complexes and, especially to provide stabilization of the low oxidation states. We report here magnetization hysteresis for those complexes at low temperature over at least three redox states, proving for the first time the SMM behavior of the dianionic and trianionic states of a Pc_2Ln complex, which extends the range of studied oxidation states for Ln = Tb from $(-1/0/+1)$[38] to $(-1/-2/-3)$.

EXPERIMENTAL SECTION

All reagents were used as received from commercial sources. UV−visible absorption spectra were collected on a Varian Cary 5000 spectrometer at one data point every 0.66 nm and measured at a scan rate of 1200 nm·min^{-1}; the bandwidth was 2.0 nm, and the averaging time was 0.033 s. Cyclic voltammetric studies were carried out using a VersaSTAT 3 potentiostat from Princeton Applied Research. Standard cyclic voltammetry was carried out using a three-electrode arrangement in a single compartment cell. A glassy carbon working electrode, a Pt wire secondary electrode and a silver wire as a pseudo-reference electrode were used. The potentials were then calibrated with ferrocene/ferrocenium couple as an internal reference with $E_{1/2}$ = 0.48 V vs SCE in acetone.[52] The samples for solid-state magnetometry consisted of gelatin capsules filled with the powdered samples. Ac-magnetic susceptibility measurements were performed on a Quantum Design PPMS magnetometer, and for magnetization hysteresis, the samples were mounted on a vibrating sample magnetometer (VSM). The UV−vis spectroelectrochemical experiments were carried out with an optically transparent electrochemical (OTE) cell (modified quartz cuvette; optical path length, 0.5 mm).[53] A three-electrode configuration consisting of a Pt gauze working electrode, a Pt wire secondary electrode, and a Ag/AgCl reference electrode chemically isolated from the test solution via bridge tube containing electrolyte solution and terminated in a porous frit was used. The potential at the working electrode was controlled by the VersaSTAT 3 potentiostat. EPR spectra were recorded on a Bruker ELEXYS E500 X-band spectrometer equipped with a field-frequency (F/F) lock accessory and built-in NMR gaussmeter. A rectangular TE102 cavity was used for the measurements. The signal-to-noise ratio of spectra was increased by accumulation of scans using the F/F lock accessory to guarantee large field reproducibility. Precautions to avoid undesirable spectral distortions and line broadenings, such as those arising from microwave power saturation and magnetic field over modulation, were also taken. To avoid dipolar line broadening from dissolved oxygen, solutions were always carefully degassed with pure argon. MCD spectra were recorded on a JASCO J-810 spectropolarimeter with a bandwidth of 1 nm, and a response time of 1 s (i.e., a time constant of 0.25 s) that was adapted to incorporate an Oxford Instruments Spectromag SM4000 magnetocryostat. The samples solutions were loaded into cells of ca. 2 mm path length constructed from quartz discs separated by a Teflon spacer and frozen in liquid nitrogen.

dx.doi.org/10.1021/ic3027418 | Inorg. Chem. 2013, 52, 4464−4471

RESULTS AND DISCUSSION

Fluorinated Double-Decker Phthalocyanine Lanthanide Complexes. The complexes employ the 1,4,8,11,15,18,22,25-octakis-fluoro-2,3,9,10,16,17,23,24-octakis-perfluoro(isopropyl)phthalocyanine ligand (Figure 2a), which has been shown to yield mononuclear complexes that resist electron loss.[43,48] The solid-state structures of the mononuclear perfluorinated metal complexes have been described in detail[43] and are essentially invariable, with the metal centers being located at the center of the fluorinated macrocycle.

Pc_2Ln complexes form via the one-pot reaction of the appropriate fluorinated precursor[54] with a lanthanide salt, followed by chromatographic separations and crystallizations. Single crystals suitable for X-ray diffraction have been obtained, and the structures have been solved. The results are shown in Figure 2.[55] $\mathbf{1_{Ln}H}$ appear to contain $\mathbf{1_{Ln}}^-$ (see below), with the charge compensated by a proton that is most likely disordered over the eight aza nitrogen atoms of the Pc rings.[55] Complexes $\mathbf{1_{Ln}H}$ exhibit the classic sandwich arrangement of Pc_2Ln complexes,[56] including the dome distortions of the ligands, and represent the first halogenated double-decker complexes prepared to date.

Electrochemistry and Spectroelectrochemistry of $\mathbf{1_{Tb}}$. Pc_2Ln complexes usually present a rich electrochemistry[57,58] and may exhibit up to five reduction and two oxidation processes.[58] The redox properties of $\mathbf{1_{Tb}H}$ were studied by cyclic voltammetry using 0.5 mM solutions of $\mathbf{1_{Tb}H}$ in acetone containing 0.1 M $[TBA][PF_6]$ as electrolyte. All potentials are referenced to SCE. A total of five redox processes were observed for $\mathbf{1_{Tb}H}$ (Red1−5) at 1.58, 0.14, −0.21, −0.67, and −1.10 V (Figure 3). The processes at 0.14 and −0.21 V are reversible, on the basis of comparisons with the standard Fc^+/Fc couple. The processes at +1.58, −0.67, and −1.10 V are quasi-reversible.

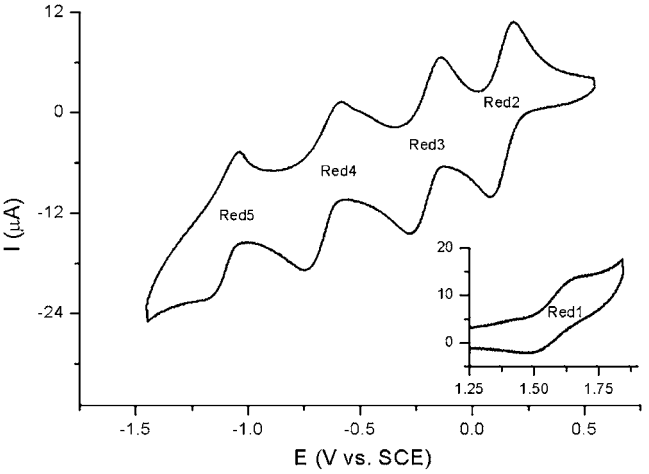

Figure 3. Cyclic voltammogram at 100 $mV \cdot s^{-1}$ of solutions of $\mathbf{1_{Tb}H}$ in acetone with $[TBA][PF_6]$ (0.1 M) as the supporting electrolyte. Inset shows a view of the oxidation region.

For $\mathbf{1_{Tb}H}$, the 64 fluorine atoms of each phthalocyanine ligand induce significant changes in the redox behavior of $\mathbf{1_{Tb}H}$ relative to the unsubstituted Pc_2Tb.[58] The perturbation induced by the fluorine atoms is such that the as-isolated $\mathbf{1_{Tb}H}$ species contain anionic $\mathbf{1_{Tb}}^-$, with a first reduction potential Red1 at 1.58 V and a second reduction Red2 at ca. 0.14 V. These potentials are ca.1.2 to 1.5 V higher than those of non-substituted or alkoxy-substituted Pc_2Ln complexes (see Table 1).[58]

Table 1. Comparison of the Redox Potentials of $\mathbf{1_{Tb}}$ in Acetone Containing 0.1 M $[TBA][PF_6]$ and Reported Values for the Non-halogenated Complex in Dichloromethane Containing 0.1 M $[TBA][PF_6]$[58a]

compd	Ox1	Red1	Red2	Red3	Red4	Red5
$\mathbf{1_{Tb}}$		+1.58	+0.14	−0.21	−0.67	−1.10
$[TBA][Pc_2Tb]$	+0.51	+0.09	−1.08	−1.32	−1.53	−1.66

[a]The potentials are quoted vs SCE.

Similar effects have been observed previously for $F_{64}PcZn$ relative to PcZn[45] in which the perfluoroalkyl groups are efficient electron-withdrawing substituents through a σ pathway from the Pc ring. These substitutions have an advantage over fluorine substituents directly bound to the Pc ring where π-donation from the fluorine substituents competes with electron withdrawal through a σ pathway. The redox processes are summarized in Scheme 1.

Scheme 1. One-Electron Redox Processes of $\mathbf{1_{Tb}}$

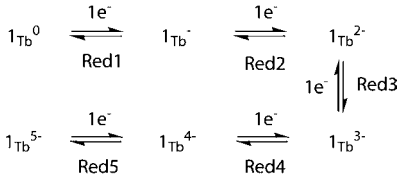

The changes in the UV−vis spectra of solutions of $\mathbf{1_{Tb}H}$ that accompany the redox processes detailed in Scheme 1 were examined by spectroelectrochemistry using an optically transparent electrode (Figure 4). While detailed spectroscopic information exists for nonsubstituted neutral, reduced, and oxidized double-decker complexes,[59] only limited spectroelectrochemistry experiments have been performed on doubly and triply reduced states.[60] The dianionic species $\mathbf{1_{Tb}}^{2-}$ could be generated from the anionic compound $\mathbf{1_{Tb}}^-$ by applying a potential of −0.12 V vs SCE. In the Q-band region, the band at 682 nm of $\mathbf{1_{Tb}}^-$ gradually disappeared to give rise to a new band at 645 nm with a shoulder at 694 nm. Two new bands are formed at 452 and 495 nm, in the π-radical region of the spectrum, demonstrating the injection of an unpaired electron in the π-system of the complex. The split Soret band of $\mathbf{1_{Tb}}^-$ joins in a single broad band at 360 nm. Finally, in the NIR region, the band around 860 nm assigned to a vibronic transition of the split Q-band disappears to yield a new band at 920 nm, while an intervalence band appears around 1200 nm, consistent with a mixed valence state.

The trianionic moiety $\mathbf{1_{Tb}}^{3-}$ could be obtained, in turn, by the reduction of $\mathbf{1_{Tb}}^{2-}$ at a potential of −0.55 V vs SCE. The reduction is evidenced by the strong increase of the relative intensity of the band at 452 nm that characterizes π-radical regions, in contrast to the band at 495 nm whose intensity is virtually unchanged. Moreover, the Q-band splits further to yield two bands at 620 and 697 nm, while in the NIR region a new band appears at 1500 nm and grows at the expense of the intervalence band observed at 1200 nm (Figure 5).

Taken together, the UV−vis spectral changes support the assignments of the electrochemical processes outlined above (Scheme 1). The spectra of the starting material and the

dx.doi.org/10.1021/ic3027418 | Inorg. Chem. 2013, 52, 4464−4471

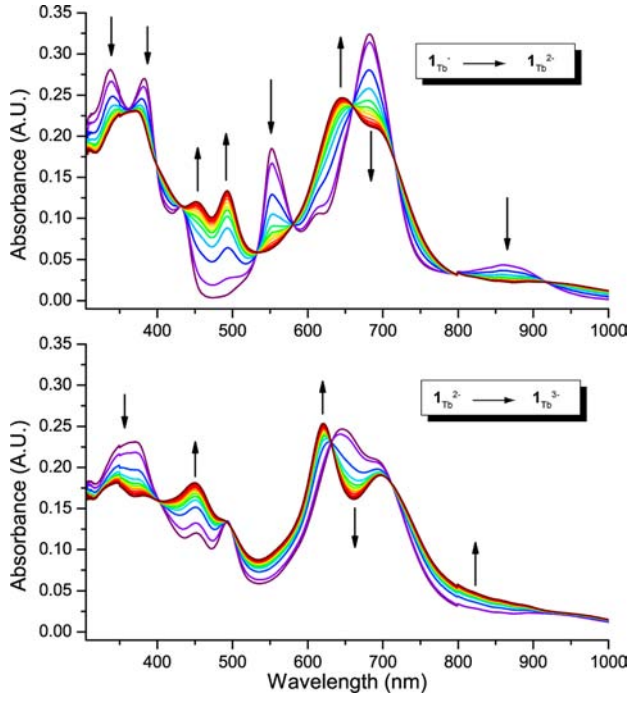

Figure 4. Successive UV−vis spectra recorded during the electrochemical reduction of an acetone solution of $\mathbf{1}_{Tb}^{-}$ to yield $\mathbf{1}_{Tb}^{2-}$ by applying a potential of −0.12 V vs SCE (top) and the reduction of $\mathbf{1}_{Tb}^{2-}$ to $\mathbf{1}_{Tb}^{3-}$ by applying a potential of −0.55 V vs SCE (bottom). [TBA][PF_6] (0.1 M) was the supporting electrolyte.

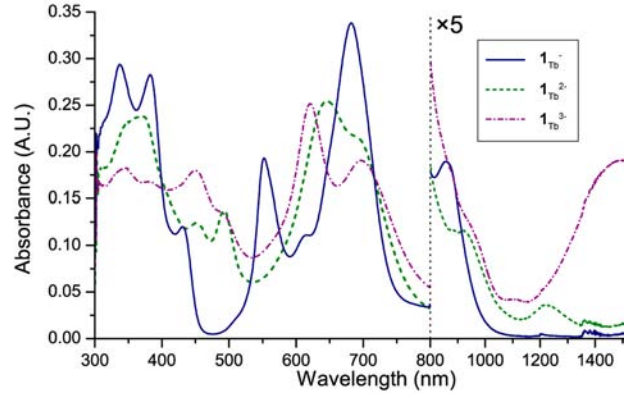

Figure 5. UV−vis absorption spectra of acetone solutions of $\mathbf{1}_{Tb}^{-}$ containing [TBA][PF_6] (0.1 M) and of $\mathbf{1}_{Tb}^{2-}$ and $\mathbf{1}_{Tb}^{3-}$ generated electrochemically from $\mathbf{1}_{Tb}^{-}$.

regenerated species were essentially identical, thus demonstrating the chemical reversibility of the redox process. The UV−vis spectra of $\mathbf{1}_{Tb}^{-}$, $\mathbf{1}_{Tb}^{2-}$, and $\mathbf{1}_{Tb}^{3-}$ are shown in Figure 5. It is worth noting here that, as observed for perfluorinated single-decker complexes,[45] the absorption spectra of all three redox states differ strongly from nonsubstituted literature precedents.[60]

Electron paramagnetic resonance. Both UV−vis and electrochemical data support that the resting states of $\mathbf{1}_{Tb}^{-}$ complexes contain two Pc^{2-} ligands, as opposed to the usual $Pc^{2-}Pc^{\bullet-}$ electronic configuration of neutral Pc_2Ln complexes (see Table 2).

This assignment is less evident for the single-crystal X-ray structure of $\mathbf{1}_{Tb}\mathbf{H}$, in which a proton cannot be identified reliably and in which differences in bond distances and angles

Table 2. Electronic Structure of the Different Redox States of the [Pc_2Lu] Species and Expected EPR Activity

redox state	electronic structure	EPR active
+1	$(Pc^{\bullet-})Lu^{3+}(Pc^{\bullet-})$	no (coupled ligand spins)
0	$(Pc^{2-})Lu^{3+}(Pc^{\bullet-})$	yes
−1	$(Pc^{2-})Lu^{3+}(Pc^{2-})$	no (no ligand spin)
−2	$(Pc^{\bullet3-})Lu^{3+}(Pc^{2-})$	yes
−3	$(Pc^{\bullet3-})Lu^{3+}(Pc^{\bullet3-})$	no (coupled ligand spins)

for Pc_2Ln may be borderline statistically significant.[55] Electron paramagnetic resonance experiments were performed considering that the reduction processes, if correctly assigned, should generate alternatively paramagnetic EPR-active and EPR-silent diamagnetic species for the isostructural $\mathbf{1}_{Lu}$ complex that also contains a nonreducible but diamagnetic metal center (see Table 2). Furthermore, for the putative resting $Pc^{2-}Pc^{\bullet-}$ electronic configuration, potentially present in the neutral $(F_{64}Pc^{2-})(F_{64}Pc^{\bullet-})Lu^{3+}$ complex, the EPR spectrum should reveal a feature at ca. g = 2.00 with narrow line width.[61,62] No EPR signal could be obtained at room temperature from a solution of $\mathbf{1}_{Lu}$ in acetone containing 0.2 M [TBA][PF_6] as supporting electrolyte. On the other hand, the X-band EPR spectrum of a frozen solution of the initial sample of $\mathbf{1}_{Lu}$ in acetone with [TBA][PF_6] (0.2 M) recorded at 150 K, showed only a weak asymmetric feature at g = 2.0021 with a line width of ca. 9 G (see Figure 6).

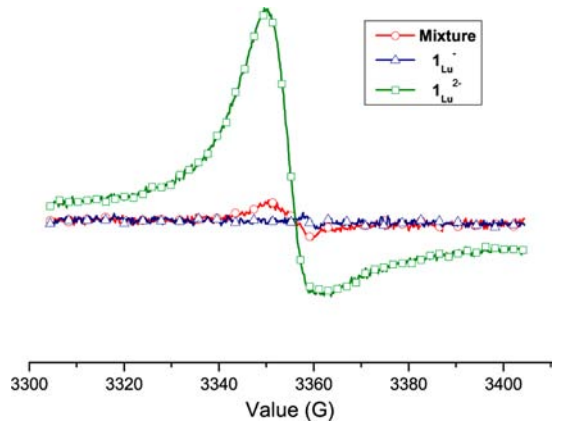

Figure 6. EPR spectra of $\mathbf{1}_{Lu}^{-}$, $\mathbf{1}_{Lu}^{2-}$ and the nonelectrolyzed sample containing a mixture of these two redox states at 150 K.

This weak signal was attributed to traces of $\mathbf{1}_{Lu}^{2-}$, which was confirmed by the presence of a the π-radical band of $\mathbf{1}_{Lu}^{2-}$ at 495 nm in the UV−vis spectrum of the initial $\mathbf{1}_{Lu}^{-}$ sample. The sample was therefore reoxidized at 0.5 V vs SCE for ca. 30 min to ensure a pure $\mathbf{1}_{Lu}^{-}$ composition (i.e., to ensure that the transformation of the traces of paramagnetic $Pc^{\bullet3-}$ into diamagnetic Pc^{2-} is complete), which was confirmed by the disappearance of the 495 nm band. The reoxidized sample (see Figure 6) was EPR silent, as expected for the closed-shell anionic species. Furthermore, $\mathbf{1}_{Lu}^{2-}$ was prepared by the bulk electrolysis of a $\mathbf{1}_{Lu}^{-}$ solution at −0.16 V vs SCE for 1 h. As anticipated, this process resulted in the appearance of an EPR signal at g = 2.0021, with an asymmetrical line shape and a line width of ca. 12 G.

Taken together, the UV−vis and EPR data establish $\mathbf{1}_{Ln}^{-}$ (Ln = Tb, Lu) as the resting state of the complexes in solution, also lending support to the X-ray data that are unable to indicate

dx.doi.org/10.1021/ic3027418 | Inorg. Chem. 2013, 52, 4464−4471

directly the presence of a disordered proton. No EPR line could be observed for $\mathbf{1}_{Tb}$ or for the other terbium double-decker compound used in our previous studies,[38] which is probably due to the strong coupling between the ligand spins and the lanthanide ion in those complexes.[63]

Bulk Magnetic Measurements. The typical behaviors of single-molecule magnets include the appearance of frequency-dependent peaks in temperature-dependent ac-magnetic susceptibility measurements and a slow magnetization relaxation, which translates into the occurrence of magnetization hysteresis at low temperature.[1] The ac-magnetic susceptibility of $\mathbf{1}_{Tb}\mathbf{H}$ was recorded at frequencies between 10 and 10000 Hz and at temperatures ranging from 10 to 60 K. In the absence of a dc offset field, the ac-susceptibility peaks were very broad due to the efficient tunneling of magnetization in $\mathbf{1}_{Tb}\mathbf{H}$. The measurements were, therefore, repeated with a 1 T dc offset field in order to detune the m_J states of $\mathbf{1}_{Tb}\mathbf{H}$ and to disable the tunneling pathway. Under these conditions (Supporting Information, S1–4), the ac magnetic susceptibility plots clearly exhibited frequency-dependent maxima, which could be fitted to Debye processes with a Cole–Cole model (Supporting Information, S3).[64] The Arrhenius analysis of the relaxation time (Figure 7) shows that the magnetic relaxation of

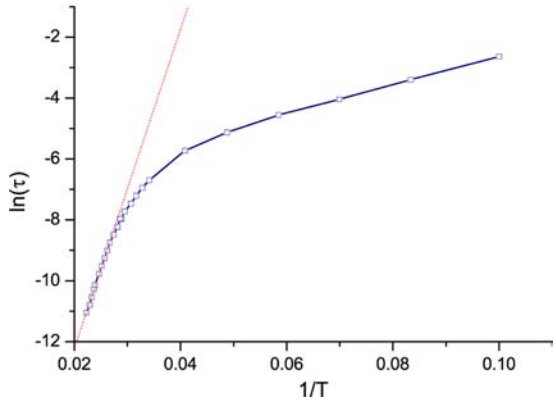

Figure 7. Arrhenius plot of the natural logarithm of the relaxation time of $\mathbf{1}_{Tb}\mathbf{H}$ as a function of $1/T$. The dashed line corresponds to the linear fit of the thermally activated Orbach regime at high temperatures.

$\mathbf{1}_{Tb}\mathbf{H}$ is similar to that of other Pc_2Tb compounds[30,33,38,65,66] and follows a thermally activated Orbach process at high temperatures with a pre-exponential factor $\tau_0^{-1} = 1.33 \times 10^{-10}$ and an activation barrier $\Delta = 365$ cm^{-1}.

While the pre-exponential factor is similar to that of unsubstituted double-decker terbium complexes, the activation barrier is slightly lower than that of Pc_2Tb ($\Delta = 420$ cm^{-1}).[29]

Magnetization hysteresis measurements were also performed on a polycrystalline powder sample of as-isolated $\mathbf{1}_{Tb}\mathbf{H}$ at 2 K and at a scan rate of 1 T·min^{-1}. The resulting hysteresis curve (Supporting Information, S5) exhibits the typical butterfly shaped hysteresis that has been observed previously for substituted and unsubstituted Pc_2Dy and Pc_2Tb complexes.[7,38,66]

Magnetic Circular Dichroism. The magnetization of the Tb complexes in solution was studied using magnetic circular dichroism (MCD) spectroscopy, a technique that has been shown to be a powerful tool for revealing SMM behavior.[14,15,38] A dilute solution of $\mathbf{1}_{Tb}\mathbf{H}$ in acetone containing 0.8 M [TBA][PF_6] was prepared (the concentration of electrolyte was increased in order to obtain on freezing a glass with good optical properties), and solutions of $\mathbf{1}_{Tb}^-$, $\mathbf{1}_{Tb}^{2-}$, and $\mathbf{1}_{Tb}^{3-}$ were generated from it by controlled electrolysis at potentials (determined previously from spectroelectrochemical experiments) 0.37 (to ensure the conversion of the trace amount of $\mathbf{1}_{Tb}^{2-}$ to $\mathbf{1}_{Tb}^-$), −0.03, and −0.47 V vs SCE, respectively. After the electrolysis was complete, the samples were injected into a sample cell and frozen in liquid nitrogen prior to insertion into the spectrometer. The identity of each species was confirmed by a comparison of the low temperature *in situ* absorption spectra and the room temperature spectra recorded in the spectroelectrochemical experiments (see Supporting Information, Figures S13–S15). The *in situ* absorption spectrum of each frozen solution sample of $\mathbf{1}_{Tb}^-$, $\mathbf{1}_{Tb}^{2-}$, and $\mathbf{1}_{Tb}^{3-}$ corresponds, essentially, to the room-temperature spectra for each complex. A splitting of the broad Q-band at 682 into two bands at 703 and 660 nm was observed for $\mathbf{1}_{Tb}^-$, which was attributed to an increase in resolution of these bands at low temperature. These UV–vis spectroscopic results support the absence of aggregation of the samples under the conditions used. The low-temperature MCD spectra of frozen solutions of $\mathbf{1}_{Tb}^-$, $\mathbf{1}_{Tb}^{2-}$, and $\mathbf{1}_{Tb}^{3-}$ are shown in Figure 8.

The MCD spectrum of $\mathbf{1}_{Tb}^-$ is dominated by two pseudo-A terms corresponding to the split Q-band at 700 and 661 nm in the low-temperature UV–vis spectrum (Figure S13, Supporting Information), and a second pseudo-A term at 552 nm. For $\mathbf{1}_{Tb}^{2-}$, the band at 700 nm in the UV–vis spectrum (Figure S14, Supporting Information) gives rise to an absorption

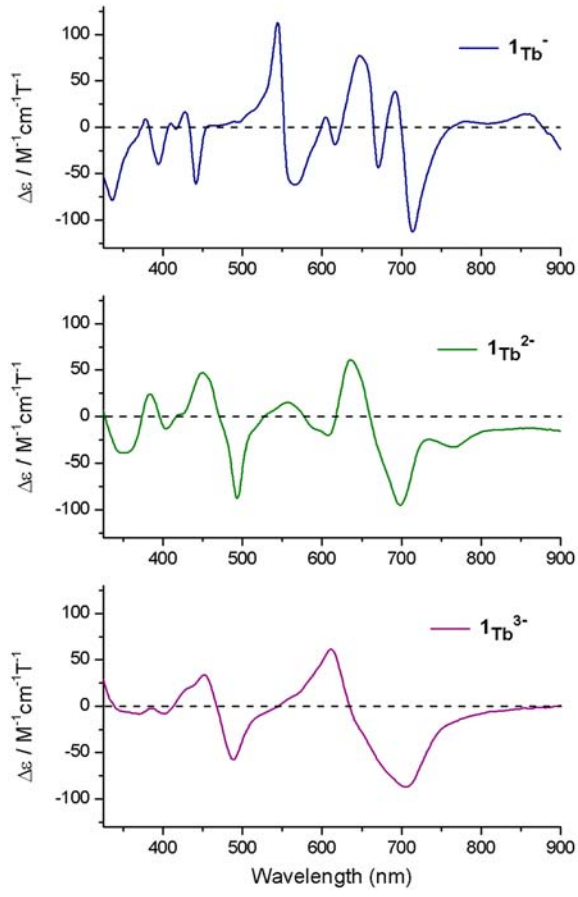

Figure 8. MCD spectra of solutions of $\mathbf{1}_{Tb}^-$, $\mathbf{1}_{Tb}^{2-}$, and $\mathbf{1}_{Tb}^{3-}$ at 3 K and 7 T in acetone with [TBA][PF_6].

dx.doi.org/10.1021/ic3027418 | Inorg. Chem. 2013, 52, 4464–4471

shaped MCD term while the band at 621 nm appears as a pseudo-A term. The Q-band of $\mathbf{1}_{Tb}^{3-}$ yields two absorption-shaped terms of opposite sign at 705 and 610 nm. Finally, the fingerprint π-radical band of both $\mathbf{1}_{Tb}^{2-}$ and $\mathbf{1}_{Tb}^{3-}$ show intense temperature-dependent negative MCD terms at 494 and 488 nm, respectively.

Magnetization experiments in solution at 1.8 K were performed by monitoring the intensity of the MCD terms in the MCD spectra of $\mathbf{1}_{Tb}^{-}$, $\mathbf{1}_{Tb}^{2-}$, and $\mathbf{1}_{Tb}^{3-}$. Since significant overlap of different terms is possible, care was taken to select bands that were well isolated from one another to obtain the magnetization hysteresis curves. Thus, the MCD intensity was measured at 562, 494, and 705 nm for $\mathbf{1}_{Tb}^{-}$, $\mathbf{1}_{Tb}^{2-}$, and $\mathbf{1}_{Tb}^{3-}$, respectively, while sweeping the magnetic field between −2 T and +2 T at a sweep rate of 1 T·min^{-1}.

The magnetization hysteresis curves are shown in Figure 9. The curves for both $\mathbf{1}_{Tb}^{-}$ and $\mathbf{1}_{Tb}^{3-}$, measured at 562 and 705 nm, respectively, display butterfly shaped hysteresis (i.e., hysteresis loops that narrow down close to zero-field), a feature that is quite common for the double-decker lanthanide species.[7,29] The narrowing of the loops occurs at B < 0.1 T, and

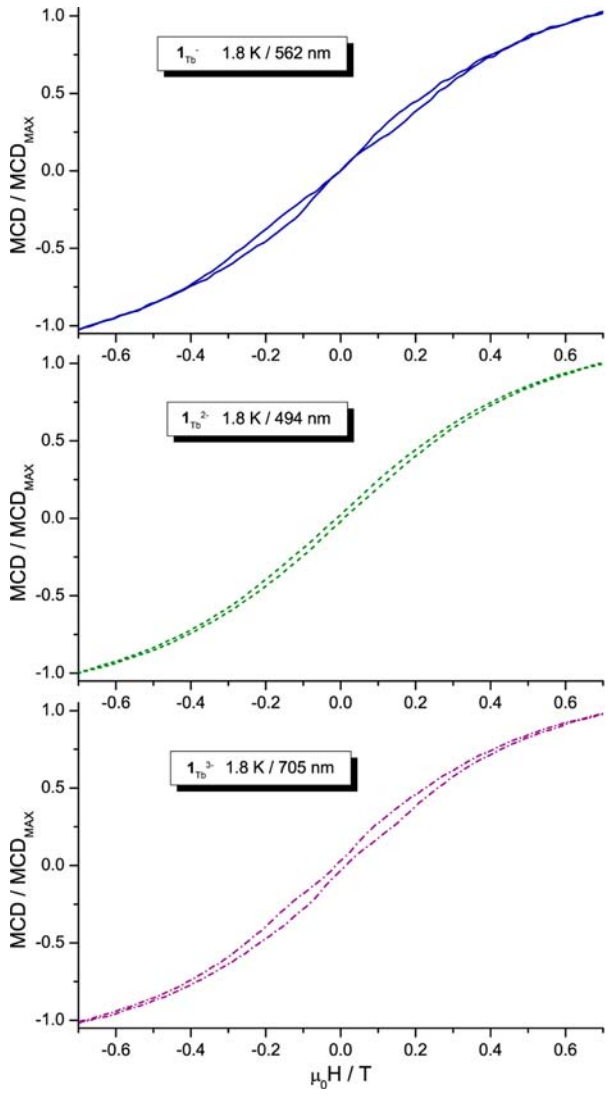

Figure 9. Hysteresis curves of the normalized MCD intensity recorded at 1.8−1.9 K and at a sweep rate of 1 T·min^{-1} for $\mathbf{1}_{Tb}^{-}$ (top), $\mathbf{1}_{Tb}^{2-}$ (middle), and $\mathbf{1}_{Tb}^{3-}$ (bottom).

can be attributed to the occurrence of quantum tunneling of magnetization at small field values between the different $|Jz\rangle|Iz\rangle$ states in $\mathbf{1}_{Tb}^{-}$ and $\mathbf{1}_{Tb}^{3-}$.[7] In contrast, the field-dependent MCD intensity of the Q-band of $\mathbf{1}_{Tb}^{2-}$ shows an open loop without any notable narrowing close to zero-field. This suggests that the tunneling regime is not as efficient in $\mathbf{1}_{Tb}^{2-}$ as in the other redox states in frozen solution.

In an earlier study, the field-dependent MCD intensities of the cationic, neutral, and anionic states of a Pc_2Tb complex were recorded under similar conditions.[38] In that case, the anionic and cationic double-decker complex also presented butterfly hysteresis, while the neutral complex presented an open loop hysteresis. Thus, it appears that for Pc_2Tb complexes the odd charged redox states (i.e., +1, −1, and −3) present a butterfly shaped hysteresis while the even charged redox states (i.e., 0 and −2) present an open loop hysteresis. The latter case coincides with the even charged redox states of Pc_2Lu being EPR-active, that is, those complexes possessing unpaired electrons within the Pc π-system.

Thus, the radical nature of the ligands in the neutral and dianionic states of Pc_2Ln may play a role in the deactivation of the tunnelling regime, which may be due to the coupling that is known to exist between the lanthanide f orbitals and the ligand spin in lanthanide double-decker complexes.[63]

CONCLUSIONS

A new double-decker Pc_2Ln single-molecule magnet, the first representative of fluorinated SMMs, has been characterized. The perfluorination of the phthalocyanine ligands led to unconventional complexes that do not contain hydrogen atoms and which exhibits rich electrochemistry. This has permitted the magnetic characterization of super-reduced Pc_2Ln species for the first time. The magnetic properties of $\mathbf{1}_{Tb}^{-}$, $\mathbf{1}_{Tb}^{2-}$, and $\mathbf{1}_{Tb}^{3-}$ significantly extend the number of characterized redox states to a total of five, from −3 to +1, for Pc_2Tb species. Furthermore our results confirm and extend a trend suggested in our previous studies,[38] in which the profile of the magnetization hysteresis is a function of the parity of the redox state of the Pc_2Tb complex. We attribute this trend to the partial quenching of the quantum tunnelling of magnetization in species where the central lanthanide ion is coordinated by organic radical containing ligands. There are several potential explanations for this effect, including the coupling between the ligand spins and the lanthanide f orbitals, as well as the Kramers doublet nature of the even number redox states (i.e., $\mathbf{1}_{Tb}^{0}$ and $\mathbf{1}_{Tb}^{2-}$), in which no electronic spin tunnelling is possible. The latter result could prove to be a crucial tool to control the quantum tunneling of magnetization in these and related complexes.

ASSOCIATED CONTENT

Supporting Information

$\chi'(T)$, $\chi''(T)$, $\chi'(\nu)$, $\chi''(\nu)$, M (T), Cole−Cole plot, cyclic voltammetry, additional spectroelectrochemistry, comparison of frozen samples and UV−vis reference data, and additional MCD spectra. This material is available free of charge via the Internet at http://pubs.acs.org.

AUTHOR INFORMATION

Corresponding Author

*E-mail addresses: sergiu.gorun@shu.edu (S.M.G.), vecianaj@icmab.es (J.V.).

dx.doi.org/10.1021/ic3027418 | Inorg. Chem. 2013, 52, 4464−4471

Notes

The authors declare no competing financial interest.

■ ACKNOWLEDGMENTS

S.G.M. thanks Mr. W. Graham (U.S.A.) for providing samples of the double-decker complexes and N. Ishikawa and W. Wernsdorfer for sharing unpublished results. J.V., J.V-G., and M.G. thank Isaac Alcon (ICMAB, Barcelona) for recording a few UV−vis spectra and the DGI (Spain) for the project POMAS CTQ2010-19501/BQU, the Networking Research Center on Bioengineering, Biomaterials and Nanomedicine (CIBER-BBN), and Generalitat de Catalunya (grant 2009SGR00516). S.M.G. thanks the National Science Foundation and the Department of Defense (U.S.A.) for financial support.

■ REFERENCES

(1) Gatteschi, D.; Sessoli, R.; Villain, J. *Molecular Nanomagnets*; Oxford University Press: Oxford, U.K., 2006.
(2) Lehmann, J.; Gaita-Arino, A.; Coronado, E.; Loss, D. *J. Mater. Chem.* **2009**, *19*, 1672.
(3) Affronte, M. *J. Mater. Chem.* **2009**, *19*, 1731.
(4) Ardavan, A.; Blundell, S. J. *J. Mater. Chem.* **2009**, *19*, 1754.
(5) Bogani, L.; Wernsdorfer, W. *Nat. Mater.* **2008**, *7*, 179.
(6) Camarero, J.; Coronado, E. *J. Mater. Chem.* **2009**, *19*, 1678.
(7) Ishikawa, N.; Sugita, M.; Wernsdorfer, W. *Angew. Chem., Int. Ed.* **2005**, *44*, 2931.
(8) Gatteschi, D.; Sessoli, R. *Angew. Chem., Int. Ed.* **2003**, *42*, 268.
(9) Luis, F.; Mettes, F. L.; Tejada, J.; Gatteschi, D.; de Jongh, L. J. *Phys. Rev. Lett.* **2000**, *85*, 4377.
(10) Rogez, G.; Donnio, B.; Terazzi, E.; Gallani, J.-L.; Kappler, J.-P.; Bucher, J.-P.; Drillon, M. *Adv. Mater.* **2009**, *21*, 4323.
(11) Mannini, M.; Sainctavit, P.; Sessoli, R.; Cartier dit Moulin, C.; Pineider, F.; Arrio, M. A.; Cornia, A.; Gatteschi, D. *Chem.—Eur. J.* **2008**, *14*, 7530.
(12) Awaga, K.; Suzuki, Y.; Hachisuka, H.; Takeda, K. *J. Mater. Chem.* **2006**, *16*, 2516.
(13) Naitabdi, A.; Bucher, J.-P.; Gerbier, P.; Rabu, P.; Drillon, m. *Adv. Mater.* **2005**, *17*, 1612.
(14) Domingo, N.; Williamson, B. E.; Gomez-Segura, J.; Gerbier, P.; Ruiz-Molina, D.; Amabilino, D. B.; Veciana, J.; Tejada, J. *Phys. Rev. B* **2004**, *69*, No. 052405.
(15) McInnes, E. J. L.; Pidcock, E.; Oganesyan, V. S.; Cheesman, M. R.; Powell, A. K.; Thomson, A. J. *J. Am. Chem. Soc.* **2002**, *124*, 9219.
(16) Aubin, S. M. J.; Sun, Z.; Eppley, H. J.; Rumberger, E. M.; Guzei, I. A.; Folting, K.; Gantzel, P. K.; Rheingold, A. L.; Christou, G.; Hendrickson, D. N. *Inorg. Chem.* **2001**, *40*, 2127.
(17) Bhattacharjee, A.; Miyazaki, Y.; Nakano, M.; Yoo, J.; Christou, G.; Hendrickson, D. N.; Sorai, M. *Polyhedron* **2001**, *20*, 1607.
(18) Wernsdorfer, W.; Caneschi, A.; Sessoli, R.; Gatteschi, D.; Cornia, A.; Villar, V. V.; Paulsen, C. *Phys. Rev. Lett.* **2000**, *84*, 2965.
(19) Barra, A. L.; Gatteschi, D.; Sessoli, R. *Chemistry* **2000**, *6*, 1608.
(20) Bradley, J. M.; Thomson, A. J.; Inglis, R.; Milios, C. J.; Brechin, E. K.; Piligkos, S. *Dalton Trans.* **2010**, *39*, 9904.
(21) Milios, C. J.; Inglis, R.; Bagai, R.; Wernsdorfer, W.; Collins, A.; Moggach, S.; Parsons, S.; Perlepes, S. P.; Christou, G.; Brechin, E. K. *Chem. Commun.* **2007**, 3476.
(22) Milios, C. J.; Inglis, R.; Vinslava, A.; Bagai, R.; Wernsdorfer, W.; Parsons, S.; Perlepes, S. P.; Christou, G.; Brechin, E. K. *J. Am. Chem. Soc.* **2007**, *129*, 12505.
(23) Vidal-Gancedo, J.; Minguet, M.; Luneau, D.; Amabilino, D. B.; Veciana, J. *J. Phys. Chem. Solids* **2004**, *65*, 723.
(24) Boskovic, C.; Bircher, R.; Tregenna-Piggott, P. L.; Gudel, H. U.; Paulsen, C.; Wernsdorfer, W.; Barra, A. L.; Khatsko, E.; Neels, A.; Stoeckli-Evans, H. *J. Am. Chem. Soc.* **2003**, *125*, 14046.
(25) Aubin, S. M. J.; Dilley, N. R.; Pardi, L.; Krzystek, J.; Wemple, M. W.; Brunel, L.-C.; Maple, M. B.; Christou, G.; Hendrickson, D. N. *J. Am. Chem. Soc.* **1998**, *120*, 4991.
(26) Freedman, D. E.; Harman, W. H.; Harris, T. D.; Long, G. J.; Chang, C. J.; Long, J. R. *J. Am. Chem. Soc.* **2010**, *132*, 1224.
(27) AlDamen, M. A.; Cardona-Serra, S.; Clemente-Juan, J. M.; Coronado, E.; Gaita-Ariño, A.; Martí-Gastaldo, C.; Luis, F.; Montero, O. *Inorg. Chem.* **2009**, *48*, 3467.
(28) Ishikawa, N.; Sugita, M.; Ishikawa, T.; Koshihara, S.-Y.; Kaizu, Y. *J. Am. Chem. Soc.* **2003**, *125*, 8694.
(29) Ishikawa, N.; Sugita, M.; Ishikawa, T.; Koshihara, S.-Y.; Kaizu, Y. *J. Phys. Chem. B* **2004**, *108*, 11265.
(30) Ishikawa, N. *Polyhedron* **2007**, *26*, 2147.
(31) Ishikawa, N.; Sugita, M.; Okubo, T.; Tanaka, N.; Iino, T.; Kaizu, Y. *Inorg. Chem.* **2003**, *42*, 2440.
(32) Mannini, M.; Tancini, E.; Sorace, L.; Sainctavit, P.; Arrio, M.-A.; Qian, Y.; Otero, E.; Chiappe, D.; Margheriti, L.; Cezar, J. C.; Sessoli, R.; Cornia, A. *Inorg. Chem.* **2011**, *50*, 2911.
(33) Gonidec, M.; Biagi, R.; Corradini, V.; Moro, F.; De Renzi, V.; del Pennino, U.; Summa, D.; Muccioli, L.; Zannoni, C.; Amabilino, D. B.; Veciana, J. *J. Am. Chem. Soc.* **2011**, *133*, 6603.
(34) Biagi, R.; Fernandez-Rodriguez, J.; Gonidec, M.; Mirone, A.; Corradini, V.; Moro, F.; De Renzi, V.; del Pennino, U.; Cezar, J. C.; Amabilino, D. B.; Veciana, J. *Phys. Rev. B* **2010**, *82*, No. 224406.
(35) Stepanow, S.; Honolka, J.; Gambardella, P.; Vitali, L.; Abdurakhmanova, N.; Tseng, T.-C.; Rauschenbach, S.; Tait, S. L.; Sessi, V.; Klyatskaya, S.; Ruben, M.; Kern, K. *J. Am. Chem. Soc.* **2010**, *132*, 11900.
(36) Vitali, L.; Fabris, S.; Conte, A. M.; Brink, S.; Ruben, M.; Baroni, S.; Kern, K. *Nano Lett.* **2008**, *8*, 3364.
(37) Ishikawa, N.; Sugita, M.; Wernsdorfer, W. *J. Am. Chem. Soc.* **2005**, *127*, 3650.
(38) Gonidec, M.; Davies, E. S.; McMaster, J.; Amabilino, D. B.; Veciana, J. *J. Am. Chem. Soc.* **2010**, *132*, 1756.
(39) Takamatsu, S.; Ishikawa, T.; Koshihara, S.-Y.; Ishikawa, N. *Inorg. Chem.* **2007**, *46*, 7250.
(40) Takamatsu, S.; Ishikawa, N. *Polyhedron* **2007**, *26*, 1859.
(41) Ishikawa, N.; Sugita, M.; Tanaka, N.; Ishikawa, T.; Koshihara, S.-Y.; Kaizu, Y. *Inorg. Chem.* **2004**, *43*, 5498.
(42) Lee, H.-J.; Brennessel, W. W.; Lessing, J. A.; Brucker, W. W.; Young, V. G., Jr.; Gorun, S. M. *Chem. Commun.* **2003**, 1576.
(43) Bench, B. A.; Beveridge, A.; Sharman, W. M.; Diebold, G. J.; Lier, J. E. v.; Gorun, S. M. *Angew. Chem., Int. Ed.* **2002**, *41*, 747.
(44) Łapok, Ł.; Lener, M.; Tsaryova, O.; Nagel, S.; Keil, C.; Gerdes, R.; Schlettwein, D.; Gorun, S. M *Inorg. Chem.* **2011**, *50*, 4086.
(45) Keizer, S. P.; Mack, J.; Bench, B. A.; Gorun, S. M.; Stillman, M. J. *J. Am. Chem. Soc.* **2003**, *125*, 7067.
(46) Moons, H.; Łapok, Ł.; Loas, A.; Van Doorslaer, S.; Gorun, S. M. *Inorg. Chem.* **2010**, *49*, 8779.
(47) Nagel, S.; Lener, M.; Keil, C.; Gerdes, R.; Łapok, Ł.; Gorun, S. M.; Schlettwein, D. *J. Phys. Chem. C* **2011**, *115*, 8759.
(48) Bench, B. A.; Brennessel, W. W.; Lee, H.-J.; Gorun, S. M. *Angew. Chem., Int. Ed.* **2002**, *41*, 750.
(49) Schlothauer, J. C.; Hackbarth, S.; Jäger, L.; Drobniewski, K.; Patel, H.; Gorun, S. M.; Röder, B. *J. Biomed. Opt.* **2012**, *17*, No. 115005.
(50) Beveridge, A. C.; Bench, B. A.; Gorun, S. M.; Diebold, G. J. *J. Phys. Chem. A* **2003**, *107*, 5138.
(51) Loas, A.; Gerdes, R.; Zhang, Y.; Gorun, S. M. *Dalton Trans.* **2011**, *40*, 5162.
(52) Connelly, N. G.; Geiger, W. E. *Chem. Rev.* **1996**, *96*, 877.
(53) Macgregor, S. A.; McInnes, E.; Sorbie, R. J.; Yellowlees, L. J. In *Molecular Electrochemistry of Inorganic, Bioinorganic and Organometallic Compounds*; Pombeiro, A. J. L., McCleverty, J. A., Eds.; Kluwer Academic Publishers: Dordrecht, the Netherlands, 1993; p 503.
(54) Gorun, S. M.; Bench, B. A.; Carpenter, G.; Beggs, M. W.; Mague, J. T.; Ensley, H. E. *J. Fluorine Chem.* **1998**, *91*, 37.
(55) Gorun, S. M. et al. Manuscript in preparation.

(56) De Cian, A.; Moussavi, M.; Fischer, J.; Weiss, R. *Inorg. Chem.* **1985**, *24*, 3162.
(57) Kadish, K. M.; Nakanishi, T.; Gurek, A.; Ahsen, V.; Yilmaz, I. *J. Phys. Chem. B* **2001**, *105*, 9817.
(58) Zhu, P.; Lu, F.; Pan, N.; Arnold, Dennis P.; Zhang, S.; Jiang, J. *Eur. J. Inorg. Chem.* **2004**, *2004*, 510.
(59) Ishikawa, N. *J. Porphyrins Phthalocyanines* **2001**, *5*, 87.
(60) Yilmaz, I.; Nakanishi, T.; Gürek, A.; Kadish, K. M. *J. Porphyrins Phthalocyanines* **2003**, *07*, 227.
(61) Chang, A. T.; Marchon, J.-C. *Inorg. Chim. Acta* **1981**, *53*, L241.
(62) Corker, G. A.; Grant, B.; Clecak, N. J. *J. Electrochem. Soc.* **1979**, *126*, 1339.
(63) Trojan, K. L.; Kendall, J. L.; Kepler, K. D.; Hatfield, W. E. *Inorg. Chim. Acta* **1992**, *198*−*200*, 795.
(64) Cole, K. S.; Cole, R. H. *J. Chem. Phys.* **1941**, *9*, 341.
(65) Gonidec, M.; Luis, F.; Vílchez, À.; Esquena, J.; Amabilino, David B.; Veciana, J. *Angew. Chem., Int. Ed.* **2010**, *49*, 1623.
(66) Waters, M.; Moro, F.; Krivokapic, I.; McMaster, J.; Slageren, J. v. *Dalton Trans.* **2012**, *41*, 1128.